

# Future Circular Collider Based Lepton-Hadron and Photon-Hadron Colliders: Luminosity and Physics

Y. C. Acar,<sup>\*</sup> A. N. Akay,<sup>†</sup> S. Beser,<sup>‡</sup> and B. B. Oner<sup>§</sup>  
*TOBB University of Economics and Technology, Ankara, Turkey*

H. Karadeniz<sup>¶</sup>  
*Giresun University, Giresun, Turkey*

U. Kaya<sup>\*\*</sup>  
*TOBB University of Economics and Technology, Ankara, Turkey and  
 Ankara University, Ankara, Turkey*

S. Sultansoy<sup>††</sup>  
*TOBB University of Economics and Technology, Ankara, Turkey and  
 ANAS Institute of Physics, Baku, Azerbaijan*

Construction of future electron-positron colliders (or dedicated electron linac) and muon colliders (or dedicated muon ring) tangential to Future Circular Collider (FCC) will give opportunity to utilize highest energy proton and nucleus beams for lepton-hadron and photon-hadron collisions. Luminosity values of FCC based  $ep$ ,  $\mu p$ ,  $eA$ ,  $\mu A$ ,  $\gamma p$  and  $\gamma A$  colliders are estimated. Multi-TeV center of mass energy  $ep$  colliders based on the FCC and linear colliders (LC) are considered in detail. Parameters of upgraded versions of the FCC proton beam are determined to optimize luminosity of electron-proton collisions keeping beam-beam effects in mind. Numerical calculations are performed using a currently being developed collision point simulator. It is shown that  $L_{ep} \sim 10^{32} \text{ cm}^{-2} \text{ s}^{-1}$  can be achieved with LHeC-like upgrade of the FCC parameters.

## I. INTRODUCTION

During last decades colliders have provided most of our knowledge on fundamental constituents of matter and their interactions. Particle colliders can be classified concerning center-of-mass energy, colliding beams and collider types:

- Collider types: ring-ring, linac-linac and linac-ring,
- Center-of-mass energy: energy frontiers and particle factories,
- Colliding beams: hadron, lepton, photon, lepton-hadron and photon-hadron colliders.

The ring-ring colliders are the most advanced from technology viewpoint and are widely used around the world. As for the linac-linac colliders, essential experience is handled due to SLC (Stanford Linear Collider [1] with  $\sqrt{s} = 0.1 \text{ TeV}$ ) operation and ILC/CLIC (International Linear Collider project [2] with  $\sqrt{s} = 0.5 - 1 \text{ TeV}$  / Compact Linear Collider project [3] with  $\sqrt{s}$  up to  $3 \text{ TeV}$ )

related studies. The linac-ring colliders are less familiar (for history of linac-ring type collider proposals see [4]).

In Table I we present correlations between colliding beams and collider types for energy frontier colliders where symbol “+” implies that given type of collider provides maximal center of mass energy for this type of colliding particles (for example; linac-ring type colliders will give opportunity to achieve highest center of mass energy for  $ep$  collisions). Concerning the center-of-mass energy: hadron colliders provide highest values (for this reason they are considered as "discovery" machines), while lepton colliders have an order smaller  $E_{CM}$ , and lepton-hadron colliders provide intermediate  $E_{CM}$ . It should be mentioned that differences in center-of-mass energies become fewer at partonic level. From the BSM search point of view, lepton-hadron colliders are comparable with hadron colliders and essentially exceeds potential of lepton colliders for a lot of new phenomena (see [5] for LHC (Large Hadron Collider [6] with  $\sqrt{s} = 14 \text{ TeV}$  at

Table I. Energy frontier colliders: colliding beams vs collider types.

Colliders	Ring-Ring	Linac-Linac	Linac-Ring
Hadron	+		
Lepton ( $e^-e^+$ )		+	
Lepton ( $\mu^-\mu^+$ )	+		
Lepton-hadron ( $eh$ )			+
Lepton-hadron ( $\mu h$ )	+		
Photon-hadron			+

<sup>\*</sup> ycacar@etu.edu.tr

<sup>†</sup> aakay@etu.edu.tr

<sup>‡</sup> sbeser@etu.edu.tr

<sup>§</sup> b.oner@etu.edu.tr

<sup>¶</sup> hande.karadeniz@giresun.edu.tr

<sup>\*\*</sup> ukaya@etu.edu.tr

<sup>††</sup> ssultansoy@etu.edu.tr

CERN), CLIC and LEP@LHC (Large Electron Positron Collider [7] with  $\sqrt{s} = 0.1 - 0.2$  TeV at CERN) comparison and [8] for LHC, ILC and ILC@LHC comparison).

Below we list past and future energy frontier colliders for three time periods (Tevatron [9] denotes  $\bar{p}p$  collider with  $\sqrt{s} = 1.98$  TeV at FNAL, HERA [10] denotes  $\sqrt{s} = 0.3$  TeV  $ep$  collider at DESY, low energy  $\mu C$  denotes Muon Collider project [11] with  $\sqrt{s} = 0.126$  TeV, LHeC denotes  $\sqrt{s} = 1.3$  TeV  $ep$  collider project [12], PWFA-LC denotes Plasma Wake-Field Accelerator-Linear Collider project [13], high energy  $\mu C$  denotes Muon Collider project [11] with  $\sqrt{s}$  up to 3 TeV):

- Before the LHC (<2010): Tevatron ( $\bar{p}p$ ), SLC/LEP ( $e^-e^+$ ) and HERA ( $ep$ ),
- LHC era (2010-2030): LHC ( $pp$ ,  $AA$ ), ILC ( $e^-e^+$ ), low energy  $\mu C$  ( $\mu^-\mu^+$ ), LHeC ( $ep$ ,  $eA$ ) and  $\mu$ -LHC ( $\mu p$ ,  $\mu A$ ),
- After the LHC (>2030): FCC ( $pp$ ,  $AA$ ), CLIC ( $e^-e^+$ ), PWFA-LC ( $e^-e^+$ ), high energy  $\mu C$  ( $\mu^-\mu^+$ ), and FCC based lepton-hadron and photon-hadron colliders, namely,  $e$ -FCC ( $ep$ ,  $eA$ ) and  $\mu$ -FCC ( $\mu p$ ,  $\mu A$ ) and  $\gamma$ -FCC ( $\gamma p$ ,  $\gamma A$ ).

Comparison of contemporary lepton and hadron colliders shows that hadron colliders have much higher center of mass energies even at partonic level. Therefore, formers give opportunity to search for heavier new particles and/or probe smaller distances. This is why they are called “discovery” machines.

It is known that lepton-hadron scattering had played crucial role in our understanding of deep inside of matter. For example, electron scattering on atomic nuclei reveals structure of nucleons in Hofstadter experiment [14]. Moreover, quark parton model was originated from lepton-hadron collisions at SLAC [15]. Extending the kinematic region by two orders of magnitude both in high  $Q^2$  and small  $x$ , HERA (the first and still unique lepton-hadron collider) with  $\sqrt{s} = 0.32$  TeV has shown its superiority compared to the fixed target experiments and provided parton distribution functions (PDF) for LHC and Tevatron experiments. Unfortunately, the region of sufficiently small  $x$  ( $< 10^{-6}$ ) and high  $Q^2$  ( $\geq 10 \text{ GeV}^2$ ), where saturation of parton densities should manifest itself, has not been reached yet. Hopefully, LHeC [12] with  $\sqrt{s} = 1.3$  TeV will give opportunity to investigate this region.

Construction of linear  $e^+e^-$  colliders (or special linac) and muon colliders (or special muon ring) tangential to the future circular collider (FCC), as shown in Fig. 1, will give opportunity to achieve highest center of mass energy in lepton-hadron and photon-hadron collisions [16, 17].

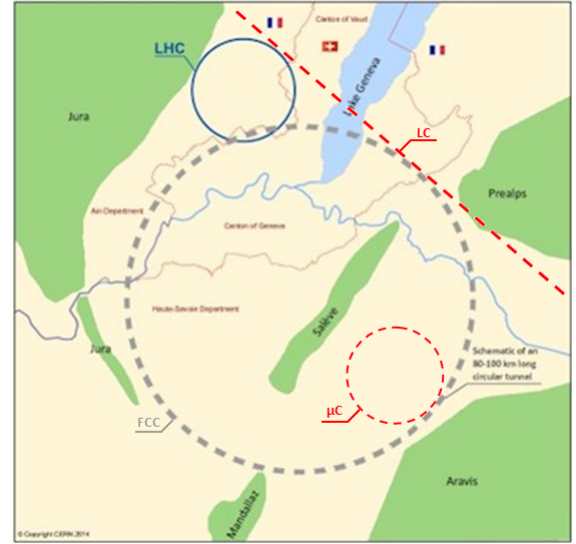


Figure 1. Possible configuration for FCC, linear collider (LC) and muon collider ( $\mu C$ ).

FCC is the future 100 TeV center-of-mass energy  $pp$  collider studied at CERN and supported by European Union within the Horizon 2020 Framework Programme for Research and Innovation [18]. Main parameters of the FCC  $pp$  option [19] are presented in Table II. The FCC also includes an electron-positron collider option in the same tunnel (TLEP) [20], as well as several  $ep$  collider options [21].

Table II. Main parameters of proton beams in FCC.

Beam Energy (TeV)	50
Peak Luminosity ( $10^{34} \text{ cm}^{-2} \text{ s}^{-1}$ )	5.6
Particle per Bunch ( $10^{10}$ )	10
Norm. Transverse Emittance ( $\mu\text{m}$ )	2.2
$\beta^*$ amplitude function at IP (m)	1.1
IP beam size ( $\mu\text{m}$ )	6.8
Bunches per Beam	10600
Bunch Spacing (ns)	25
Bunch length (mm)	80
Beam-beam parameter, $\xi_{pp}$	$5.6 \times 10^{-3}$

Energy recovery linac (ERL) with  $E_e = 60 \text{ GeV}$  is chosen as the main option for LHeC. Same ERL can also be used for FCC based  $ep$  collider [21]. Concerning  $e^-$  ring in the FCC tunnel [21] energy of electrons is limited ( $E_e < 200 \text{ GeV}$ ) due to large synchrotron radiation (synchrotron radiation power is proportional to the fourth power of energy and inversely proportional to the square of the ring radius and to the fourth power of the particle mass). Higher electron energies can be handled only by constructing linear colliders (or special linac) tangential to the FCC. For the first time this approach was proposed for UNK@VLEPP based  $ep$  colliders [22] (UNK denotes  $pp$  collider project with  $\sqrt{s} = 6$  TeV at IHEP, VLEPP denotes multi-hundred GeV  $e^+e^-$  collider at BINP). Then,

construction of TESLA tangential to HERA (THERA project) was considered [23]. This line was followed by consideration of the LC@LHC  $ep$  collider proposals (see reviews [24–26] and references therein).

In this paper, we consider main parameters of the FCC based lepton-hadron ( $lp$ ,  $lA$ ) and photon-hadron ( $\gamma p$ ,  $\gamma A$ ) colliders, especially LC@FCC based  $ep$  collider schemes. In Section II, we estimate luminosity of FCC based  $ep$  colliders taking into account beam-beam tune shift and disruption effects. In numerical calculations, we utilize main parameters of ILC (International Linear Collider) [2] and PWFA-LC (Plasma Wake Field Accelerator - Linear Collider) [13] using a simulation program under development for lepton-hadron colliders. Possible other options, namely,  $eA$ ,  $\mu p/\mu A$  and  $\gamma p/\gamma A$  are briefly discussed in Section III. In Section IV, conclusions and recommendations are presented after comparison of LC, FCC- $pp$  and LC@FCC colliders' potentials for color octet electron search.

## II. LC@FCC BASED $ep$ COLLIDERS

General expression for luminosity of FCC based  $lh$  colliders is given by ( $l$  denotes electron or muon,  $h$  denotes proton or nucleus):

$$L_{lh} = \frac{N_l N_h}{4\pi \max[\sigma_{x_h}, \sigma_{x_l}] \max[\sigma_{y_h}, \sigma_{y_l}]} \min[f_{c_h}, f_{c_l}] \quad (1)$$

where  $N_l$  and  $N_h$  are numbers of leptons and hadrons per bunch, respectively;  $\sigma_{x_h}$  ( $\sigma_{x_l}$ ) and  $\sigma_{y_h}$  ( $\sigma_{y_l}$ ) are the horizontal and vertical hadron (lepton) beam sizes at IP;  $f_{c_l}$  and  $f_{c_h}$  are LC and FCC bunch frequencies.  $f_c$  is expressed by  $f_c = N_b f_{rep}$ , where  $N_b$  denotes number of bunches,  $f_{rep}$  means revolution frequency for FCC and pulse frequency for LC. In order to determine collision frequency of  $lh$  collider, minimum value should be chosen among lepton and hadron bunch frequencies. Some of these parameters can be rearranged in order to maximize  $L_{lh}$  but one should note that there are some main limitations that should be considered. One of these limitations is lepton beam power, however only parameters of FCC hadron beam is rearranged in this study and only nominal parameters of linear colliders are considered. Therefore, there is no change of electron beam power due to upgrades. Other limitations for linac-ring type  $lh$  colliders are due to beam-beam effects. In general, a better focusing is needed to have high luminosity values at interaction points (IP). However, although an intensely focused beam including charged particles with large Lorentz factor ( $\gamma \gg 1$ ) does not have a strong influence on its internal beam particles, due to canceling of Lorentz forces one another (space charge effects diminish with  $1/\gamma^2$ ), this situation does not hold for the encountered beam. Deflection of particles under this electromagnetic interaction is called as disruption. When

this interaction causes an angular kick in opposite beam's particles, it is called beam-beam tune shift. While beam-beam tune shift affects hadron (proton, ion) and muon beams, disruption has influence on electron beams.

Disruption parameter for electron beam is given by:

$$D_{x_e} = \frac{2 Z_h N_h r_e \sigma_{z_h}}{\gamma_e \sigma_{x_h} (\sigma_{x_h} + \sigma_{y_h})} \quad (2a)$$

$$D_{y_e} = \frac{2 Z_h N_h r_e \sigma_{z_h}}{\gamma_e \sigma_{y_h} (\sigma_{y_h} + \sigma_{x_h})} \quad (2b)$$

where,  $r_e = 2.82 \times 10^{-15}$  is classical radius for electron,  $\gamma_e$  is the Lorentz factor of electron beam,  $\sigma_{x_h}$  and  $\sigma_{y_h}$  are horizontal and vertical hadron beam sizes at IP, respectively.  $\sigma_{z_h}$  is bunch length of hadron beam.  $Z_h$  denotes atomic number for ion (for electron-proton collisions  $Z_h = 1$ ). Beam-beam parameter for hadron beams is given by:

$$\xi_{x_h} = \frac{N_l r_h \beta_h^*}{2\pi \gamma_h \sigma_{x_l} (\sigma_{x_l} + \sigma_{y_l})} \quad (3a)$$

$$\xi_{y_h} = \frac{N_l r_h \beta_h^*}{2\pi \gamma_h \sigma_{y_l} (\sigma_{y_l} + \sigma_{x_l})} \quad (3b)$$

where  $r_h$  is radius of hadron (for proton it is classical radius,  $r_p = 1.54 \times 10^{-18}$ ),  $\beta_h^*$  is beta function of hadron beam at interaction point (IP),  $\gamma_h$  is the Lorentz factor of hadron beam.  $\sigma_{x_l}$  and  $\sigma_{y_l}$  are horizontal and vertical sizes of lepton beam at IP, respectively.

Considering ILC@FCC and PWFA-LC@FCC options, one should note that bunch spacing of electron accelerators are always greater than FCC, while proton beam sizes are always greater than the electron beam sizes at IP. Details and parameters of electron beam accelerators are given in further subsections. In numerical calculations, we use transversely matched electron and proton beams at IP. Keeping in mind roundness of FCC proton beam, Eqs (1)-(3) turn into;

$$L_{ep} = \frac{N_e N_p}{4\pi \sigma_p^2} f_{c_e} \quad (4)$$

$$\xi_p = \frac{N_e r_p \beta_p^*}{4\pi \gamma_p \sigma_p^2} \quad (5)$$

$$D_e = \frac{N_p r_e \sigma_{z_p}}{\gamma_e \sigma_p^2} \quad (6)$$

In order to increase luminosity of  $ep$  collisions LHeC-like upgrade of the FCC proton beam parameters have been used. Namely, number of protons per bunch is increased 2.2 times ( $2.2 \times 10^{11}$  instead of  $10^{11}$ ),  $\beta$ -function of proton beam at IP is arranged to be 11 times lower (0.1 m instead of 1.1 m) which corresponds to THERA [23] and LHeC [12] designs. Therefore, IP beam size of proton beam,  $\sigma_p$ , is decreased  $\sim 3.3$  times according to the relation  $\sigma_p = \sqrt{\varepsilon_p^N \beta_p^* / \gamma_p}$ . Details of the parameter calculations for ILC $\otimes$ FCC and PWFA-LC $\otimes$ FCC  $ep$  colliders are given in subsections II.A and II.B, respectively. Numerical calculations have been performed using a new simulation software for  $ep$  colliders which is currently being developed. Details are given in subsection II.C.

### A. ILC $\otimes$ FCC

Main parameters of ILC electron beam are given in Table III. One can see from the table that bunch spacing of ILC is 554 ns which is about 22 times greater than FCC bunch spacing of 25 ns. Therefore, most of the proton bunches turning in FCC would not participate in  $ep$  collisions unless parameters of FCC (especially bunch spacing) are rearranged. For FCC, the parameter  $N_p$  can be increased while number of bunches is decreased regarding the dissipation. Transverse beam size of proton is much greater than transverse beam size of electron for ILC $\otimes$ FCC. If beam sizes are matched, this leads  $L_{ep}$  to decrease since luminosity is inversely proportional to  $\sigma_p^2$  as can be seen from Eq. (4). To increase luminosity, upgraded value of  $\beta_p^*$  parameter is set to be 0.1 m and therefore  $\sigma_p$  to be  $2.05 \mu\text{m}$ . Calculated values of  $L_{ep}$ ,  $D_e$  and  $\xi_p$  parameters for ILC $\otimes$ FCC based  $ep$  colliders with both nominal and upgraded FCC proton beam cases are given in Table IV. In addition in Table V, disruption parameter is fixed at the limit value of  $D_e = 25$  and corresponding  $N_p$  and  $L_{ep}$  values are given.

Table III. Main parameters of electron beams in ILC [2].

Beam Energy (GeV)	250	500
Peak Luminosity ( $10^{34} \text{ cm}^{-2} \text{ s}^{-1}$ )	1.47	4.90
Particle per Bunch ( $10^{10}$ )	2.00	1.74
Norm. Horiz. Emittance ( $\mu\text{m}$ )	10.0	10.0
Norm. Vert. Emittance (nm)	35.0	30.0
Horiz. $\beta^*$ amplitude function at IP (mm)	11.0	11.0
Vert. $\beta^*$ amplitude function at IP (mm)	0.48	0.23
Horiz. IP beam size (nm)	474	335
Vert. IP beam size (nm)	5.90	2.70
Bunches per Beam	1312	2450
Repetition Rate (Hz)	5.00	4.00
Beam Power at IP (MW)	10.5	27.2
Bunch Spacing (ns)	554	366
Bunch length (mm)	0.300	0.225

Table IV. Main parameters of ILC $\otimes$ FCC based  $ep$  collider.

Nominal FCC				
$E_e(\text{GeV})$	$\sqrt{s}(\text{TeV})$	$L_{ep}, \text{ cm}^{-2} \text{ s}^{-1}$	$D_e$	$\xi_p$
250	7.08	$2.26 \times 10^{30}$	1.0	$1.09 \times 10^{-3}$
500	10.0	$2.94 \times 10^{30}$	0.5	$9.40 \times 10^{-4}$
Upgraded FCC				
$E_e(\text{GeV})$	$\sqrt{s}(\text{TeV})$	$L_{ep}, \text{ cm}^{-2} \text{ s}^{-1}$	$D_e$	$\xi_p$
250	7.08	$55.0 \times 10^{30}$	24	$1.09 \times 10^{-3}$
500	10.0	$70.0 \times 10^{30}$	12	$9.40 \times 10^{-4}$

Table V. Main parameters of ILC $\otimes$ FCC based  $ep$  collider corresponding to the disruption limit  $D_e = 25$ .

$E_e(\text{GeV})$	$\sqrt{s}(\text{TeV})$	$N_p(10^{11})$	$L_{ep}, \text{ cm}^{-2} \text{ s}^{-1}$	$\xi_p$
250	7.08	2.3	$57 \times 10^{30}$	$1.09 \times 10^{-3}$
500	10.0	4.6	$149 \times 10^{30}$	$9.40 \times 10^{-4}$

### B. PWFA-LC $\otimes$ FCC

Beam driven plasma wake field technology made a great progress for linear accelerators recently. This method enables an electron beam to obtain high gradients of energy even only propagating through small distances compared to the radio frequency resonance based accelerators [13]. In other words, more compact linear accelerators can be built utilizing PWFA to obtain a specified beam energy. In Table VI, main electron beam parameters of PWFA-LC accelerator are listed. As in ILC $\otimes$ FCC case, transverse beam size of proton is greater than all PWFA  $e$ -beam options. Same upgrade for the proton beam is handled ( $N_p = 2.2 \times 10^{11}$ ,  $\beta_p^* = 0.1 \text{ m}$ ) and final values of luminosity, disruption and beam-beam parameters are given in Table VII for both nominal and upgraded FCC proton beam cases. In Table VIII, disruption parameter is fixed at the limit value of  $D_e = 25$  and corresponding  $ep$  collider parameters are given.

Table VI. Main parameters of electron beams in PWFA-LC [13].

Beam Energy (GeV)	250	500	1500	5000
Peak Luminosity ( $10^{34} \text{ cm}^{-2} \text{ s}^{-1}$ )	1.25	1.88	3.76	6.27
Particle per Bunch ( $10^{10}$ )	1	1	1	1
Norm. Horiz. Emittance ( $10^{-5} \text{ m}$ )	1.00	1.00	1.00	1.00
Norm. Vert. Emittance ( $10^{-8} \text{ m}$ )	3.50	3.50	3.50	3.50
Horiz. $\beta^*$ function at IP ( $10^{-3} \text{ m}$ )	11	11	11	11
Vert. $\beta^*$ function at IP ( $10^{-5} \text{ m}$ )	9.9	9.9	9.9	9.9
Horiz. IP beam size ( $10^{-7} \text{ m}$ )	4.74	3.36	1.94	1.06
Vert. IP beam size ( $10^{-10} \text{ m}$ )	26.7	18.9	10.9	5.98
Bunches per Beam	1	1	1	1
Repetition Rate ( $10^3 \text{ Hz}$ )	20	15	10	5
Beam Power at IP (MW)	8	12	24	40
Bunch Spacing ( $10^4 \text{ ns}$ )	5.00	6.67	10.0	20.0
Bunch length ( $10^{-5} \text{ m}$ )	2.00	2.00	2.00	2.00

Table VII. Main parameters of PWFA-LC⊗FCC based  $ep$  collider.

		Nominal FCC		
$E_e(GeV)$	$\sqrt{s}(TeV)$	$L_{ep}, cm^{-2}s^{-1}$	$D_e$	$\xi_p$
250	7.08	$3.44 \times 10^{30}$	1.00	$5.47 \times 10^{-4}$
500	10.0	$2.58 \times 10^{30}$	0.50	$5.47 \times 10^{-4}$
1500	17.3	$1.72 \times 10^{30}$	0.17	$5.47 \times 10^{-4}$
5000	31.6	$0.86 \times 10^{30}$	0.05	$5.47 \times 10^{-4}$
		Upgraded FCC		
$E_e(GeV)$	$\sqrt{s}(TeV)$			
250	7.08	$82.6 \times 10^{30}$	24	$5.47 \times 10^{-4}$
500	10.0	$61.9 \times 10^{30}$	12	$5.47 \times 10^{-4}$
1500	17.3	$41.3 \times 10^{30}$	4.0	$5.47 \times 10^{-4}$
5000	31.6	$20.8 \times 10^{30}$	1.2	$5.47 \times 10^{-4}$

As one can see from the third column of the Table VIII number of protons in bunches are huge in options corresponding to the highest energy electron beams, therefore one may wonder about IBS growth times. For this reason we estimate horizontal IBS growth times using Wei formula [27]:

$$\left[ \frac{\frac{1}{\sigma_{pt}} \frac{d\sigma_{pf}}{dt}}{\frac{1}{\sigma_x} \frac{d\sigma_x}{dt}} \right] = \frac{Z^4 N r_0^2 c L_c}{8\pi A \gamma^2 \sigma_s \sigma_{pt} \beta \epsilon_x \epsilon_y} \times \frac{(1 + a^2 + b^2) I(\frac{a^2 + b^2}{2}) - 3}{1 - (\frac{a^2 + b^2}{2})} \begin{bmatrix} (1 - d^2) \\ d^2 - (a^2/2) \\ -b^2/2 \end{bmatrix} \quad (7)$$

where  $L_c$  is FODO cell length,  $a = \beta_x d / D_h \gamma$ ,  $b = (\beta_y \sigma_x / \beta_x \sigma_y) a$ ,  $d = D_h \sigma_{pf} / (\sigma_x^2 + D_h^2 \sigma_{pf}^2)^{1/2}$ ,  $\sigma_{pf}$  is the fractional momentum deviation,  $\sigma_s$  is the rms bunch length,  $\sigma_x$  and  $\sigma_y$  are horizontal and vertical amplitudes, respectively.  $D_h$  is horizontal dispersion and its average value is equal to [28, 29]:

$$\frac{L_c \theta_c}{4} \left( \frac{1}{\sin^2 \frac{\mu}{2}} - \frac{1}{12} \right) \quad (8)$$

where  $\mu$  is the phase advance. The bending angle per cell is taken as  $\theta_c = 0.79$  [19] and finally the function  $I(\chi)$  is expressed as:

$$I(\chi) = \begin{cases} \frac{1}{\sqrt{\chi(\chi-1)}} \text{Arth} \sqrt{\frac{\chi-1}{\chi}} & \chi \geq 1 \\ \frac{1}{\sqrt{\chi(\chi-1)}} \text{Arctan} \sqrt{\frac{1-\chi}{\chi}} & \chi < 1 \end{cases} \quad (9)$$

Obtained results are presented in the last two columns of the Table VIII. In numerical calculations we used FODO cell lengths values  $L_c = 106.9$  m (same as LHC) and  $L_c = 203.0$  m considered in [29]. It is seen that IBS growth times are acceptable even for  $E_e = 5000$  GeV case.

### C. Collision Point Simulator for the FCC Based lepton-hadron and photon-hadron Colliders

There are several beam-beam simulation programs for linear  $e^+e^-$  and photon colliders (see for example [30, 31]). Unfortunately, no similar programs exist for  $ep$  colliders. In order to understand and analyze electron-proton beam interactions at collision points, we start to develop a numerical program that considers beam dynamics with aim to optimize electron and proton beam parameters in order to obtain maximal luminosity values. At this stage luminosity, beam-beam tune shift, disruption and beam life-time formulae (Equations 1-3, 7-9, 12-20) are included in, and the numerical results of this paper are calculated using current software. The aim of the software is to optimize main parameters of lepton-hadron colliders. It is obvious that luminosity values with nominal beam parameters can be calculated analytically. However, when beam dynamics is deeply analyzed considering time evolution of beam structures, it becomes almost impossible to make analytical solutions. These affects become time-dependent due to varying beam sizes. The work on the upgraded version which will include time dependent behaviour of beams during collision as well as  $\gamma p$  collider options is under progress.

In addition, in order to achieve highest luminosity values at the collision, beam parameters should be optimized. For this reason an additional interface is being developed. It will optimize luminosity and give required beam parameters within predetermined parameter interval. The current version of the program is a Java based environment and therefore it is platform-independent. It is available to access at <http://alohep.hepforge.org> and our group web page ([http://yef.etu.edu.tr/ALOHEP\\_eng.html](http://yef.etu.edu.tr/ALOHEP_eng.html)).

### III. FCC BASED $\mu p$ , $eA$ , $\mu A$ , $\gamma p$ AND $\gamma A$ COLLIDERS

This section is devoted to brief discussion of additional options for FCC based  $lh$  and  $\gamma h$  colliders.

#### A. $\mu p$ Colliders

Muon-proton colliders were proposed almost two decades ago. Construction of additional proton ring in  $\sqrt{s} = 4$  TeV muon collider tunnel was suggested in [32] in order to handle  $\mu p$  collider with the same center-of-mass energy. However, luminosity value, namely  $L_{\mu p} = 3 \times 10^{35} cm^{-2} s^{-1}$ , was extremely over estimated, realistic value for this option is three orders smaller [26]. Then, construction of additional 200 GeV energy muon ring in the Tevatron tunnel in order to handle  $\sqrt{s} = 0.9$  TeV  $\mu p$  collider with  $L_{\mu p} = 10^{32} cm^{-2} s^{-1}$  was considered in [33].

In this paper we consider another design, namely, construction of muon ring close to FCC (see Fig 1). For

Table VIII. Main parameters of PWFA-LC⊗FCC based  $ep$  collider corresponding to the disruption limit  $D_e = 25$ .

$E_e(GeV)$	$\sqrt{s}(TeV)$	$N_p(10^{11})$	$L_{ep}, cm^{-2}s^{-1}$	$\xi_p$	IBS Growth Time (Horizontal) (h)	
					$L_c=106.9$ m	$L_c=203.0$ m
125	5.00	1.15	$65.0 \times 10^{30}$	$5.47 \times 10^{-4}$	721	149
250	7.08	2.30	$86.0 \times 10^{30}$	$5.47 \times 10^{-4}$	360	75.0
500	10.0	4.60	$129 \times 10^{30}$	$5.47 \times 10^{-4}$	180	37.0
1500	17.3	13.8	$258 \times 10^{30}$	$5.47 \times 10^{-4}$	60.0	12.0
5000	31.6	45.8	$433 \times 10^{30}$	$5.47 \times 10^{-4}$	18.0	3.90

round beams general expression for the luminosity given in Eq. (1) transforms to:

$$L_{pp} = f_{pp} \frac{N_p^2}{4\pi\sigma_p^2} \quad (10)$$

$$\xi_\mu = \frac{N_p r_\mu \beta_\mu^*}{4\pi\gamma_\mu \sigma_p^2} \quad (14)$$

where  $r_\mu = 1.37 \times 10^{-17}$  m is classical muon radius.

$$L_{\mu\mu} = f_{\mu\mu} \frac{N_\mu^2}{4\pi\sigma_\mu^2} \quad (11)$$

for FCC- $pp$  and  $\mu C$ , respectively. Concerning muon-proton collisions one should use larger transverse beam sizes and smaller collision frequency values. Keeping in mind that  $f_{\mu\mu}$  is an order smaller than  $f_{pp}$ , following correlation between  $\mu p$  and  $\mu\mu$  luminosities take place:

$$L_{\mu p} = \left(\frac{N_p}{N_\mu}\right) \left(\frac{\sigma_\mu}{\max[\sigma_p, \sigma_\mu]}\right)^2 L_{\mu\mu} \quad (12)$$

Table IX. Nominal muon collider parameters [11].

$\sqrt{s}$ , TeV	0.126	1.5	3.0
Avg. Luminosity, $10^{34} cm^{-2}s^{-1}$	0.008	1.25	4.4
Circumference, km	0.3	2.5	4.5
Repetition Rate, Hz	15	15	12
$\beta^*$ , cm	1.7	1	0.5
No. muons/bunch, $10^{12}$	4	2	2
No. bunches/beam	1	1	1
Norm. Trans. Emmit., $\pi mm-rad$	0.2	0.025	0.025
Bunch length, cm	6.3	1	0.5
Beam Size at IP, $\mu m$	75	6	3
Beam beam parameter / IP, $\xi_{\mu\mu}$	0.02	0.09	0.09

Using nominal parameters of  $\mu\mu$  colliders given in Table IX, according to Eq. (12), parameters of the FCC based  $\mu p$  colliders are calculated and presented in Table X. Utilizing Eq. (3) for round beams, we obtain:

$$\xi_p = \frac{N_\mu r_p \beta_p^*}{4\pi\gamma_p \sigma_\mu^2} \quad (13)$$

Beam beam parameter for muons is given by:

Table X. Main parameters of the FCC based  $\mu p$  colliders.

Collider Name	$\sqrt{s}$ , TeV	$L_{\mu p}, cm^{-2}s^{-1}$ (Avg.)	$\xi_p$	$\xi_\mu$
$\mu 63$ -FCC	3.50	$0.2 \times 10^{31}$	$1.8 \times 10^{-3}$	$5.4 \times 10^{-4}$
$\mu 750$ -FCC	12.2	$50 \times 10^{31}$	$1.1 \times 10^{-1}$	$3.3 \times 10^{-3}$
$\mu 1500$ -FCC	17.3	$50 \times 10^{31}$	$1.1 \times 10^{-1}$	$8.3 \times 10^{-4}$

As one can see from Table X, where nominal parameters of FCC proton beam are used,  $\xi_p$  for energy frontier  $\mu p$  colliders is unacceptably high and should be decreased to 0.01. According to Eq. (13), this can be succeeded by decreasing of  $\beta_p$  and/or increasing of  $\sigma_\mu$ . For example, decreasing  $\beta_p^*$  from 1.1 m to 0.1 m (as in the upgraded option of proton beams considered in Section II) seems to solve this problem. Luminosity values presented in Table X assume simultaneous operation with  $pp$  collider. These values can be increased by an order using dedicated proton beam with larger bunch population [26].

## B. $eA$ and $\mu A$ Colliders

It is known that FCC also includes  $Pb - Pb$  collider option [18, 29]. Therefore, construction of LC and  $\mu C$  tagential to FCC will provide opportunity to handle  $e$ -Pb and  $\mu$ -Pb collisions. In order to estimate luminosity of FCC based lepton-nucleus colliders we use parameters of  $Pb$ -beam for  $p - Pb$  option from [29] presented in Table XI.

Table XI. Main parameters of  $Pb$  beam in FCC  $p$ - $Pb$  option.

Beam Energy (GeV)	4100
Peak Luminosity ( $10^{30} cm^{-2} s^{-1}$ )	1.24
Particle per Bunch ( $10^{10}$ )	1.15
Norm. Transverse Emittance ( $\mu m$ )	3.75
$\beta^*$ amplitude function at IP (m)	1.1
IP beam size ( $\mu m$ )	8.8
Bunches per Beam	432
Bunch length (mm)	80
Beam-beam parameter, $\xi_{pp}$	$3.7 \times 10^{-4}$

Luminosity, disruption and beam beam tune shift for  $e$ - $Pb$  are given by:

$$L_{ePb} = \frac{N_e N_{Pb}}{4\pi\sigma_{Pb}^2} f_{ce} \quad (15)$$

$$D_e = \frac{Z_{Pb} N_{Pb} r_e \sigma_{zPb}}{\gamma_e \sigma_{Pb}^2} \quad (16)$$

$$\xi_{Pb} = \frac{N_e r_{Pb} \beta_{Pb}^*}{4\pi\gamma_{Pb} \sigma_{Pb}^2} \quad (17)$$

respectively. In Eq. (17)  $\gamma_{Pb} = E_{Pb}/m_{Pb}$  and  $r_{Pb} = (Z_{Pb}^2/A_{Pb})r_p$ . Calculated luminosity values for LC $\otimes$ FCC based  $e$ - $Pb$  colliders are given in Table XII (here upgraded FCC means  $\beta_{Pb}^* = 0.1$  m). One can see that sufficiently high luminosities can be achieved with reasonable  $D_e$  and  $\xi_{Pb}$  values.

Table XII. Main parameters of LC $\otimes$ FCC based  $e$ - $Pb$  colliders.

Collider Name	$E_e (GeV)$	Nominal FCC		
		$L_{ep}, cm^{-2} s^{-1}$	$D_e$	$\xi_{Pb}$
ILC $\otimes$ FCC	250	$6.1 \times 10^{28}$	2.2	0.021
	500	$8.0 \times 10^{28}$	1.1	0.019
PWFA-LC $\otimes$ FCC	250	$9.4 \times 10^{28}$	2.2	0.011
	500	$7.0 \times 10^{28}$	1.1	0.011
	1500	$4.7 \times 10^{28}$	0.4	0.011
	5000	$2.3 \times 10^{28}$	0.1	0.011
Collider Name	$E_e (GeV)$	Upgraded FCC		
		$L_{ep}, cm^{-2} s^{-1}$	$D_e$	$\xi_{Pb}$
ILC $\otimes$ FCC	250	$68 \times 10^{28}$	24.5	0.021
	500	$88 \times 10^{28}$	12.2	0.019
PWFA-LC $\otimes$ FCC	250	$103 \times 10^{28}$	24	0.011
	500	$77 \times 10^{28}$	12	0.011
	1500	$51 \times 10^{28}$	4	0.011
	5000	$26 \times 10^{28}$	1.2	0.011

Luminosity and beam beam tune shifts for  $\mu$ - $Pb$  colliders are given by:

$$L_{\mu Pb} = \left(\frac{N_{Pb}}{N_\mu}\right) \left(\frac{\sigma_\mu}{max[\sigma_{Pb}, \sigma_\mu]}\right)^2 L_{\mu\mu} \quad (18)$$

$$\xi_\mu = \frac{Z_{Pb} N_{Pb} r_\mu \beta_\mu^*}{4\pi\gamma_\mu \sigma_{Pb}^2} \quad (19)$$

$$\xi_{Pb} = \frac{N_\mu r_{Pb} \beta_{Pb}^*}{4\pi\gamma_{Pb} \sigma_\mu^2} \quad (20)$$

Calculated luminosity values for  $\mu$ C $\otimes$ FCC based  $\mu$ - $Pb$  colliders with nominal parameters are given in table XIII. It is seen that nominal parameters lead to unacceptably high  $\xi_{Pb}$  values. The straightforward way to reduce  $\xi_{Pb}$  is essential decreasing of  $N_\mu$ . According to Eq. (18) this leads to corresponding decreasing of luminosity as seen from the last column of Table XIII.

Table XIII. Main parameters of  $\mu$ C $\otimes$ FCC based  $\mu$ - $Pb$  colliders.

Collider Name	$E_\mu, TeV$	Nominal parameters		
		$L_{\mu Pb}, cm^{-2} s^{-1}$ (Avg.)	$\xi_{Pb}$	$\xi_\mu$
$\mu$ 63-FCC	0.063	$1.1 \times 10^{31}$	0.1	$1.5 \times 10^{-1}$
$\mu$ 750-FCC	0.75	$1.3 \times 10^{31}$	12	$7.3 \times 10^{-3}$
$\mu$ 1500-FCC	1.5	$1.1 \times 10^{31}$	47	$1.8 \times 10^{-3}$
Collider Name	$E_\mu, TeV$	Upgraded parameters		
		$L_{\mu Pb}, cm^{-2} s^{-1}$ (Avg.)	$\xi_{Pb}$	$N_\mu$
$\mu$ 63-FCC	0.063	$110 \times 10^{28}$	0.01	$4 \times 10^{11}$
$\mu$ 750-FCC	0.75	$1.1 \times 10^{28}$	0.01	$1.67 \times 10^9$
$\mu$ 1500-FCC	1.5	$0.23 \times 10^{28}$	0.01	$4.26 \times 10^8$

### C. $\gamma p$ and $\gamma A$ Colliders

In 1980's, the idea of using high energy photon beams, obtained by Compton backscattering of laser light off a beam of high energy electrons, was considered for  $\gamma e$  and  $\gamma\gamma$  colliders (see review [34] and references therein). Then the same method was proposed for constructing  $\gamma p$  colliders on the base of linac-ring type  $ep$  machines in [35]. Rough estimations of the main parameters of  $\gamma p$  collisions are given in [36]. The dependence of these parameters on the distance between conversion region (CR) and interaction point (IP) was analyzed in [31], where some design problems were considered.

It should be noted that  $\gamma p$  colliders are unique feature of linac-ring  $ep$  colliders and could not be constructed on the base of standard ring-ring type  $ep$  machines (for arguments see [36, 37]). Concerning FCC based  $\gamma p$  colliders, center of mass energy and luminosity are ap-

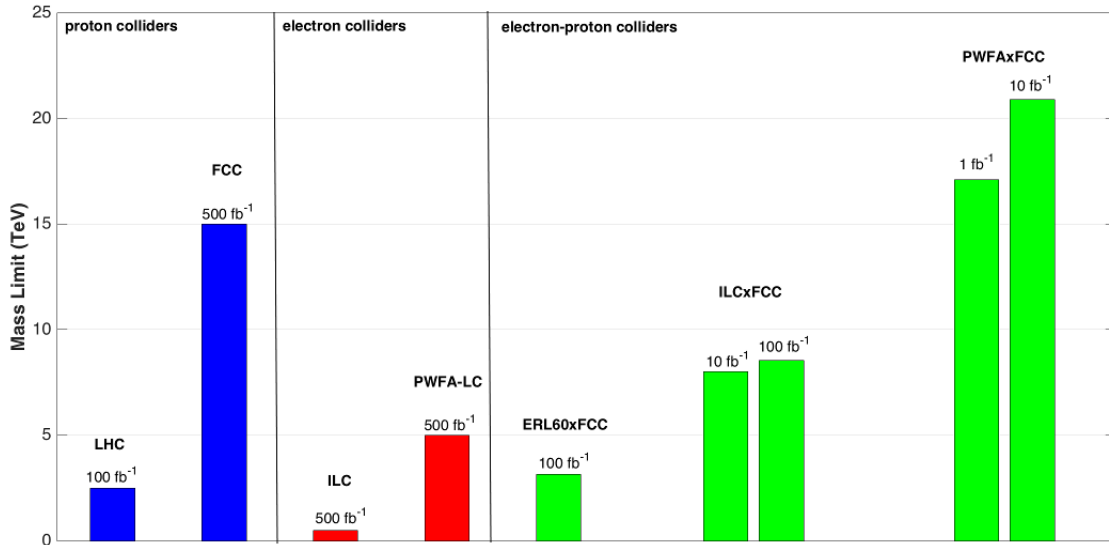


Figure 2. Discovery limits for color octet electron at different  $pp$ ,  $e^+e^-$  and  $ep$  colliders.

proximately the same as of corresponding  $ep$  colliders ( $\sqrt{s_{\gamma p}} \approx 0.9\sqrt{s_{ep}}$ ;  $L_{\gamma p} \approx L_{ep}$ ) for one-pass linacs. Let us mention that energy recovery is not effective for  $\gamma p$  colliders since electron bunches are destroyed during conversion (for details see [37]).

Regarding the analyses performed for THERA and LHeC,  $\gamma p$  colliders have shown their superiority compared to the corresponding  $ep$  colliders for a lot of SM and BSM phenomena (small  $x_g$ ,  $q^*$  and so on). Similar studies should be performed for FCC based  $\gamma p$  colliders. Certainly, FCC based  $\gamma A$  colliders will bring out great opportunities for QCD and nuclear physics research. For example,  $\gamma A$  option will give an opportunity to investigate quark-gluon plasma at very high temperatures but relatively low nuclear density (according to VMD, proposed machine will be at the same time  $\rho$ -nucleus collider).

Different aspects of the THERA based  $\gamma p$  colliders have been considered in [38]. In [39, 40] Linac@LHC based  $\gamma p$  colliders have been considered for different linac scenarios. Similar work on FCC based  $\gamma p$  and  $\gamma A$  colliders is under progress.

#### IV. CONCLUSIONS

In this study it is shown that for ILC@FCC and PWFA-LC@FCC based  $ep$  colliders, luminosity values up to  $L_{ep} \sim 10^{32} \text{ cm}^{-2} \text{ s}^{-1}$  are achievable with LHeC-like upgrade of the FCC proton beam. Even with this moderate luminosity, BSM search potential of  $ep$  colliders essentially exceeds that of corresponding linear colliders. It may also exceed the search potential of the FCC- $pp$  option for a lot of BSM phenomena. As a BSM process production of color octet electron ( $e_8$ ) at the FCC, LC@FCC

and LC have been analyzed in [41]. Mass discovery limits for  $e_8$  in  $\Lambda = M_{e_8}$  case (where  $\Lambda$  is compositeness scale) are presented in Figure 2. If FCC will discover  $e_8$ , LC@FCC will give opportunity to determine Lorentz structure of  $e_8$ -e-g vertex using longitudinal polarization of electron beam, as well as to probe compositeness scale up to hundreds TeV.

In principle, “dynamic focusing” scheme [42], which was proposed for THERA, could provide  $L_{ep} \sim 10^{33} \text{ cm}^{-2} \text{ s}^{-1}$  for all  $ep$  collider options considered in this study. Concerning ILC@FCC based  $ep$  colliders, a new scheme for energy recovery proposed for higher-energy LHeC (see Section 7.1.5 in [12]) may give an opportunity to increase luminosity by an additional one or two orders, resulting in  $L_{ep}$  exceeding  $10^{34} \text{ cm}^{-2} \text{ s}^{-1}$ . Unfortunately, this scheme can not be applied at PWFA-LC@FCC.

Acceleration of ion beams at the FCC will give opportunity to provide multi-TeV center of mass energy in electron-nucleus collisions. In addition, electron beam can be converted to high energy photon beam using Compton back-scattering of laser photons which will give opportunity to construct LC@FCC based  $\gamma p$  and  $\gamma A$  colliders.

In conclusion, construction of ILC and PWFA-LC tangential to the FCC will essentially enlarge the physics search potential for both SM and BSM phenomena. Therefore, systematic study of accelerator, detector and physics search potential, issues of LC@FCC based electron-hadron and photon-hadron colliders, as well as  $\mu C$ @FCC based muon-hadron collider, are essential to foresee the future of high energy physics. Concerning the viability of different options, ILC@FCC option seems to be the most realistic one for linac-ring type  $ep$  machine proposals, while viability of PWFA-LC@FCC and  $\mu C$ @FCC based colliders are dependent on resolution of



technical aspects of PWFA-LC and muon collider. Possible construction of dedicated  $e$ -linac and/or muon ring tangential to FCC requires separate study.

## ACKNOWLEDGMENTS

This study is supported by TUBITAK under the grant No 114F337. A. Akay and S. Sultansoy are grateful to organizers of the FCC Week 2016 for giving opportunity to present our results at this distinguished conference.

- 
- [1] SLAC Linear Collider Conceptual Design Report, SLAC-R-229, Internal report, SLAC, 1980.
  - [2] C. Adolphsen *et al.*, The International Linear Collider Technical Design Report-Volume 3. II; arXiv:1306.6328.
  - [3] M. Aicheler *et al.*, A Multi-TeV linear collider based on CLIC technology: CLIC Conceptual Design Report. Geneva, Switzerland: CERN, 2012.
  - [4] A. Akay, H. Karadeniz, and S. Sultansoy, Int. J. Mod. Phys. A **25**, 4589 (2010).
  - [5] U. Amaldi, Physics and detectors at the Large Hadron Collider and at the CERN Linear Collider, in *Workshop on Physics at Future Accelerators*, CERN Yellow report **87**, 1987 (La Thuile, Italy), p. 323.
  - [6] L. Evans and P. Bryant, LHC machine, J. Instrum. **3**, S08001 (2008).
  - [7] The LEP design report Vol. I — The LEP injector chain, CERN Report LEP/TH/83-29. The LEP design report Vol.II — The LEP main ring, CERN Report LEP/84-01. The LEP design report Vol.III — LEP2, CERN Report AC/96-01.
  - [8] S. Sultansoy, A review of TeV scale lepton-hadron and photon-hadron colliders, in *Proceedings of 2005 Particle Accelerator Conference*, 2005 (Knoxville, TN, USA), p. 4329.
  - [9] Design Report for the Tevatron I Project, FNAL, 1984.
  - [10] HERA, A Proposal for a Large Electron-Proton Beam Facility at DESY, DESY-HERA-81-10, 1981.
  - [11] J. P. Delahaye *et al.*, Enabling intensity and energy frontier science with a muon accelerator facility in the U.S., arXiv:1308.0494v2 [physics.acc-ph].
  - [12] J. L. Abelleira Fernandez *et al.* (LHeC Study Group), J. Phys. G: Nucl. Part. Phys. **39**, 075001 (2012).
  - [13] J-P. Delahaye *et al.*, A Beam Driven Plasma-Wakefield Linear Collider from Higgs Factory to Multi-TeV, in *Proceedings of the Fifth International Particle Accelerator Conference*, 2014 (Dresden, Germany), p. 3791.
  - [14] R. Hofstadter and R. W. McAllister, Phys. Rev. **98**, 217 (1955).
  - [15] J. I. Friedman and H. W. Kendall, Ann. Rev. Nucl. Sci. **2**, 203 (1972); See also the published versions of the Nobel lectures: R. E. Taylor, Rev. Mod. Phys. **6**, 573 (1991); H. W. Kendall, Rev. Mod. Phys. **6**, 597 (1991); J. I. Friedman, Rev. Mod. Phys. **6**, 615 (1991).
  - [16] Y. C. Acar, U. Kaya, B. B. Oner, and S. Sultansoy, arXiv:1510.08284v2 [hep-ex].
  - [17] Y. C. Acar, U. Kaya, B. B. Oner, and S. Sultansoy, arXiv:1602.03089 [physics.acc-ph].
  - [18] FCC web site, <https://fcc.web.cern.ch>.
  - [19] FCC pp option parameters, <https://fcc.web.cern.ch/Pages/Hadron-Collider.aspx>.
  - [20] M. Bicer *et al.* (TLEP Design Study Working Group), JHEP **1401**, 164 (2014).
  - [21] F. Zimmermann, in *KEK Accelerator Seminar*, Challenges for Highest Energy Circular Colliders, 2014 (Tsukuba, Japan).
  - [22] S. I. Alekhin *et al.*, IHEP Preprint 87-48 (1987).
  - [23] *The THERA Book*, edited by U. Katz, M. Klein, A. Levy, and S. Schlenstedt, DESY-LC-REV-2001-062 2001.
  - [24] B. H. Wiik, Recent development in accelerators, in *Proceedings of the International Europhysics Conference on High Energy Physics*, 1993 (Marseille, France), p. 739.
  - [25] R. Brinkmann *et al.*, Linac-ring type colliders: Fourth way to TeV scale, DESY preprint DESY-97-239; arXiv:physics/9712023 [physics.acc-ph].
  - [26] S. Sultansoy, The post-HERA era: brief review of future lepton-hadron and photon-hadron colliders, DESY 99-159; arXiv:hep-ph/9911417v2.
  - [27] J. Wei, Evolution of Hadron Beams under Intrabeam Scattering, in *Proceedings of 1993 Particle Accelerator Conference*, 1993 (Washington, DC, USA), p. 3653.
  - [28] *Handbook of Accelerator Physics and Engineering*, edited by A. Chao, K. Mess, M. Tigner, and F. Zimmermann, (2nd ed. World Scientific, 2013).
  - [29] M. Schaumann, Phys. Rev. ST Accel. Beams **18**, 091002 (2015); arXiv:1503.09107 [physics.acc-ph].
  - [30] D. Schulte, Beam-beam simulations with GUINEA-PIG, No. CERN-PS-99-014-LP. 1999; C. Rimbault *et al.*, GUINEA-PIG++: an upgraded version of the linear collider beam-beam interaction simulation code GUINEA-PIG., in *Proceedings of Particle Accelerator Conference* 2007, (New Mexico, USA) p.2728.
  - [31] P. Chen *et al.*, Nucl. Instrum. Meth. A **397**, 458 (1997); arXiv preprint physics/9704012.
  - [32] I. F. Ginzburg, Turk J. Phys **22**, 607 (1998).
  - [33] V. D. Shiltsev, An asymmetric muon proton collider: luminosity consideration, in *Proceedings of 1997 Particle Accelerator Conference*, 1998 (Vancouver, British Columbia, Canada), p. 420.
  - [34] V. I. Telnov, Acta. Phys. Pol. B **37**, 633 (2006).
  - [35] S. I. Alekhin *et al.*, Int. J. Mod. Phys. A **6**, 21 (1991).
  - [36] S. F. Sultanov, Prospects of the future ep and gamma p colliders: Luminosity and physics, ICTP Preprint IC/89/409, Trieste, 1989.
  - [37] A. K. Ciftci, S. Sultansoy, S. Turkoz, and O. Yavas, Nucl. Instrum. Meth. A **365**, 317 (1995).
  - [38] A.K. Ciftci, S. Sultansoy, O. Yavas, Nucl. Instrum. Meth. A **472**, 72 (2001).
  - [39] H. Aksakal, A. K. Ciftci, Z. Nergiz, D. Schulte, F. Zimmermann, Nucl. Instrum. Meth. A **576**, 287 (2007).
  - [40] H. Aksakal, A. K. Ciftci, Z. Nergiz, D. Schulte, F. Zimmermann, Luminosity Upgrade of CLIC LHC ep/ $\gamma$ p Collider, *Proceedings of Particle Accelerator Conference (PAC 07)*, 2007 (Albuquerque, New Mexico), p 2853.

- [41] Y. C. Acar, U. Kaya, B. B. Oner, and S. Sultansoy, Color octet electron search potential of the FCC based e-p colliders; arXiv:1605.08028v2 [hep-ph].
- [42] R. Brinkmann and M. Dohlus, A method to overcome the bunch length limitations on  $\beta_p^*$  for electron-proton colliders, DESY-M-95-11 1995.